


ORIGINAL ARTICLE

Identification and characterization of the binding sequences and target genes of p53 lacking the 1st transactivation domain

Shiori Suzuki^{1,2} | Shuichi Tsutsumi³ | Yu Chen¹ | Chikako Ozeki¹ | Atsushi Okabe^{3,4} | Tatsuya Kawase¹ | Hiroyuki Aburatani³ | Rieko Ohki¹ 

¹Laboratory of Fundamental Oncology, National Cancer Center Research Institute, Tokyo, Japan

²Department of Electrical Engineering and Bioscience, Graduate School of Advanced Science and Engineering, Waseda University, Tokyo, Japan

³Genome Science Division, Research Center for Advanced Science and Technology, The University of Tokyo, Tokyo, Japan

⁴Department of Molecular Oncology, Graduate School of Medicine, Chiba University, Chiba, Japan

Correspondence

Rieko Ohki, Laboratory of Fundamental Oncology, National Cancer Center Research Institute, Tsukiji 5-1-1, Chuo-ku, Tokyo 104-0045, Japan.

Email: rohki@ncc.go.jp

Funding information

Ministry of Education, Culture, Sports, Science and Technology of Japan (Grant/Award Number: 19K16732), the Ministry of Education, Culture, Sports, Science and Technology of Japan (Grant/Award Number: 17H03587) and the Ministry of Health, Labour and Welfare.

Abstract

The tumor suppressor gene *p53* encodes a transcriptional activator that has two transactivation domains (TAD) located in its amino terminus. These two TAD can transactivate genes independently, and at least one TAD is required for p53 transactivation function. The 1st TAD (a.a. 1-40) is essential for the induction of numerous classical p53 target genes, while the second TAD (a.a. 41-61) suffices for tumor suppression, although its precise molecular function remains unclear. In this study, we comprehensively identified the sites to which p53 lacking the 1st TAD (Δ 1stTAD-p53) binds, as well as its potential target genes. We found that the binding sequences for Δ 1stTAD-p53 are divergent and include not only the canonical p53 consensus binding sequences but also sequences similar to those recognized by a number of other known transcription factors. We identified and analyzed the functions of three Δ 1stTAD-p53 target genes, *PTP4A1*, *PLK2* and *RPS27L*. All three genes were induced by both full-length p53 and Δ 1stTAD-p53, and were dependent on the transactivation activity of the 2nd TAD. We also found that two of these, *PTP4A1* and *PLK2*, are endoplasmic reticulum (ER) stress-inducible genes. We found that upon ER stress, *PTP4A1* suppresses apoptosis while *PLK2* induces apoptosis. These results reveal a novel Δ 1stTAD-p53 downstream pathway that is dependent on the transcription activation activity of the 2nd TAD.

KEYWORDS

endoplasmic reticulum stress, p53, p53 isoform, Suzuki, transactivation domain, tumor suppressor

1 | INTRODUCTION

The tumor suppressor gene *p53* is one of the most frequently mutated genes in human cancer and encodes a transcriptional activator that induces a number of genes involved in tumor suppression. It is believed that this transactivation function mediates

its tumor suppression function, thereby maintaining the integrity of the cell.^{1,2} The p53 protein may be divided into three functional domains: the amino (N)-terminal domain, the central core DNA-binding domain and the carboxy-terminal domain.^{3,4} The N-terminal domain is required for p53 the transcriptional activity and consists of two transactivation domains (TAD) and a

Suzuki, Tsutsumi and Chen equally contributed to this work.

This is an open access article under the terms of the Creative Commons Attribution-NonCommercial License, which permits use, distribution and reproduction in any medium, provided the original work is properly cited and is not used for commercial purposes.

© 2019 The Authors. *Cancer Science* published by John Wiley & Sons Australia, Ltd on behalf of Japanese Cancer Association.

proline-rich domain. These two TAD can transactivate genes independently, and at least one of the two TAD is required for p53 transcriptional activity.⁵

One of the reported p53 isoforms is p47, which is an N-terminally deleted isoform whose translation initiates at an internal start codon at amino acids 40 or 44, and, therefore, lacks the 1st TAD.⁶⁻¹² This isoform is also referred to as p44, p53/p47, Δ Np53, Δ 40p53 or Δ 1stTAD-p53, the last of which is the designation we use in this manuscript. This isoform was the first identified isoform of p53 and is produced by alternative translation or splicing.⁷⁻¹¹ The existence of an endogenously expressed p53 lacking the 1st TAD raises the possibility that this protein has a specific endogenous role in tumor suppression.

Overexpression of Δ 1stTAD-p53 results in the induction of apoptosis under basal conditions and induces G2 arrest under endoplasmic reticulum (ER) stress conditions, both in a manner dependent on the transcriptional activity of the protein.^{13,14} Studies using genetically engineered mice have shown that the activity of the 1st TAD (mapped within a.a. 1-40) is essential for the induction of numerous classical p53 target genes, cell cycle arrest and apoptosis, while the activity of the second TAD (mapped within a.a. 41-61) suffices for the induction of senescence and tumor suppression.^{15,16} In addition, transgenic mice overexpressing Δ 1stTAD show phenotypes of premature aging and growth suppression.¹⁷ Furthermore, expression of Δ 1stTAD-p53 is correlated with better survival in sporadic cancer patients, consistent with its ability to induce apoptosis and to transactivate its target genes.¹⁸ Previously, we and others have reported that the patterns of p53 target gene induction are different between full-length p53 (FL-p53) and Δ 1stTAD-p53.^{7,12,18} In addition, it has been reported that the transactivation functions of FL-p53 and Δ 1stTAD-p53 differ due to their recruitment of different coactivators: p300 and TAF1.¹⁸⁻²⁰ These data collectively demonstrate that Δ 1stTAD-p53 exerts its tumor-suppressive activity through the transcriptional activation of its target genes. However, there has been no comprehensive and/or detailed analysis of Δ 1stTAD-p53 binding sequences or target genes.

In this report, we identified binding sites and genes targeted by Δ 1stTAD-p53 using microarray expression analysis, ChIP-seq and ChIP-chip analysis. We next analyzed the functions of three Δ 1stTAD-p53 target genes, *PTP4A1*, *PLK2* and *RPS27L*. All three genes were induced by both FL-p53 and Δ 1stTAD-p53, and two of them (*PTP4A1* and *PLK2*) were found to be ER stress-inducible genes. We also found that following ER stress, *PTP4A1* suppresses apoptosis while *PLK2* functions in the induction of apoptosis. These results reveal a novel Δ 1stTAD-p53 downstream pathway that is dependent on the transcription activation activity of the 2nd TAD.

2 | MATERIALS AND METHODS

For further detailed experimental procedures, please see Appendix S1 Supplemental Materials and Methods.

2.1 | Western blotting analysis

Cells were lysed in lysis buffer containing 50 mmol/L Tris-HCl (pH 8.0), 1% NP40, 250 mmol/L NaCl, 50 mmol/L NaF, 1 mmol/L Na_3VO_4 , 1 mmol/L protease inhibitor (PMSF, aprotinin and leupeptin) and 1 mmol/L DDT. Whole-cell lysates were subjected to protein quantification and analyzed by western blotting.

2.2 | Construction of recombinant adenovirus expressing Δ 1stTAD-p53, *PLK2* and *PTP4A1*

Recombinant adenovirus constructs were made as described previously^{21,22} using the Adenovirus Expression Vector Kit (Dual Version) and adenovirus genome DNA-TPC (TaKaRa) kit.

2.3 | Reverse transcription and real-time PCR

RNA was prepared using an RNeasy Mini Kit (QIAGEN) or total RNA Extraction Kit (RBC Real Genomics). Reverse transcription was carried out as previously described using total RNA (0.5-1 μ g).^{23,24} Reverse-transcribed cDNA were analyzed as previously described.^{23,24}

3 | RESULTS

3.1 | Comprehensive analysis of binding sites and genes induced by Δ 1stTAD-p53

As shown in Figure S1, HCT116 *p53*^{-/-} cells are derived from HCT116 *p53*^{+/+} cells by replacing the p53 initiation Met located in exon 2 with the initiation Met of the neomycin or hygromycin resistance gene. As a result, expression of FL-p53 is lost while that of Δ 1stTAD-p53 is retained in these cells.^{11,14} It has been reported that the same gene targeting was performed against RKO *p53*^{+/+} cells and RKO *p53*^{-/-} cells express Δ 1stTAD-p53 but not FL-p53.¹⁸ As shown in Figure 1A-C, FL-p53 expression was mainly detected in HCT116 *p53*^{+/+} cells, while strong expression of Δ 1stTAD-p53 was detected in HCT116 *p53*^{-/-} cells. We also found that the size of endogenously expressed Δ 1stTAD-p53 in HCT116 *p53*^{-/-} cells completely matched the size of ectopically expressed Δ 1stTAD-p53 (data not shown). Expression of these two variants can be distinguished by the polyclonal anti-p53 antibody FL393, which recognizes various regions of p53, and the monoclonal anti-p53 antibody DO-1, which recognizes a.a. 20-25 of p53 (Figure 1A). It has been reported that Δ 1stTAD-p53 expression is upregulated upon cytotoxic stress.^{11,14} As shown in Figure 1B,C, nutrient deprivation (FBS or Ser/Gly deprivation) or ER stress (thapsigargin, TG treatment) had little effect on FL-p53 levels but resulted in elevated Δ 1stTAD-p53 expression levels. We further subjected HCT116 *p53*^{+/+} and *p53*^{-/-} cells to serum deprivation for 24 and

48 hours and observed that FL-p53 levels were slightly decreased while $\Delta 1\text{stTAD-p53}$ levels were increased (Figure 1D).

To comprehensively identify $\Delta 1\text{stTAD-p53}$ binding sites, we performed ChIP-seq analysis using the polyclonal anti-p53 antibody FL393 in HCT116 *p53*^{-/-} cells. To enhance our detection of $\Delta 1\text{stTAD-p53}$ binding sites, we subjected cells to serum deprivation, which upregulates $\Delta 1\text{stTAD-p53}$ expression. These results were compared to the previous results obtained by ChIP-seq analysis using the anti-p53 antibody FL393 in HCT116 *p53*^{+/+} cells treated with fluorouracil (5-FU). We identified 7349 regions as potential FL-p53 binding sites (in 5-FU-treated HCT116 *p53*^{+/+} cells) and 4737 regions as potential $\Delta 1\text{stTAD-p53}$ binding sites (in FBS-deprived HCT116 *p53*^{-/-} cells; Figure 1E). Among these, 1671 regions were common to both FL-p53 and $\Delta 1\text{stTAD-p53}$.

We next analyzed these binding sequences by motif analysis using HOMER software. The p53 binding motif was identified as the most common motif among de novo motifs: it was found in 52.5% of the binding sites common for both FL-p53 and $\Delta 1\text{stTAD-p53}$ (Figure 1F), and in 62.6% of the binding sites for FL-p53 only (Figure 1G). However, the $\Delta 1\text{stTAD-p53}$ binding sequences were more divergent (Figure 1H), with the most common motif among de novo motifs showing similarity to the STAT5 (5.64%), CHR-like (6.13%) and MTF1-like (5.85%) motifs. These results suggest that the binding sites for FL-p53 are mostly similar to the consensus p53 binding sequences, whereas the binding sites for $\Delta 1\text{stTAD-p53}$ may contain not only consensus p53 binding sequences but also sequences recognized by other transcription factors. However, further verification is required to determine if $\Delta 1\text{stTAD-p53}$ binds directly to these sequences and transactivates these genes.

3.2 | Identification of potential $\Delta 1\text{stTAD-p53}$ target genes

We next performed microarray gene expression analysis using HCT116 *p53*^{-/-} cells, with or without serum deprivation (three independent datasets for each condition), to identify $\Delta 1\text{stTAD-p53}$ -inducible genes. HCT116 *p53*^{+/+} cells without any treatment (three independent datasets) were also included as a sample that is nearly negative for $\Delta 1\text{stTAD-p53}$ expression. We then analyzed expression of genes selected in Figure 1E to select potential $\Delta 1\text{stTAD-p53}$ target genes using the following three criteria: (i) genes bound by $\Delta 1\text{stTAD-p53}$ (selected in Figure 1E); (ii) genes that are transcribed in HCT116 *p53*^{-/-} cells (genes with expression values greater than 100 in microarray expression analysis); and (iii) genes that are differentially expressed between HCT116 *p53*^{+/+} and *p53*^{-/-} cells or genes that are differentially expressed between FBS-deprived HCT116 *p53*^{-/-} cells and the same cells without the treatment. Three independent analyses were performed for each condition, and genes with a significant change in expression levels between the samples (*P*-values less than 0.05) were selected (shown in Table S1). Among genes that were bound by both FL-p53 and $\Delta 1\text{stTAD-p53}$, 62 were significantly increased and 40 were

decreased (Figure 1I). In contrast, among the genes that were selectively bound by $\Delta 1\text{stTAD-p53}$, 87 were significantly increased and 63 were decreased (Figure 1I). We next analyzed the possible functions of these genes using Ingenuity Pathway Analysis (IPA) software. As shown in Figure S2, the pathways delineated by genes with binding sites common for FL-p53 and $\Delta 1\text{stTAD-p53}$ and pathways delineated by genes that are selectively bound by $\Delta 1\text{stTAD-p53}$ are very different. Genes with binding sites common for FL-p53 and $\Delta 1\text{stTAD-p53}$ are involved in pyrimidine deoxyribonucleotides de novo biosynthesis I, VEGF signaling or regulation of cellular mechanics by calpain protease, while genes with binding sites specific for $\Delta 1\text{stTAD-p53}$ are involved in cell cycle regulation by BTG family proteins, HIPPO signaling, or spermine biosynthesis. Collectively, these results suggest that $\Delta 1\text{stTAD-p53}$ regulates the expression of genes that are not only shared with FL-p53 but also that are specific for $\Delta 1\text{stTAD-p53}$ in HCT116 *p53*^{-/-} cells.

3.3 | *PLK2*, *PTP4A1* and *RPS27L* are $\Delta 1\text{stTAD}$ -inducible genes

Among the potential target genes of $\Delta 1\text{stTAD-p53}$, we focused on three genes, *PLK2* (Polo-like kinase-2), *PTP4A1* (protein tyrosine phosphatase 4A) and *RPS27L* (ribosomal protein S27-like). *PLK2* and *PTP4A1* were selected as genes highly expressed in HCT116 *p53*^{-/-} cells, and *RPS27L* was selected as a gene differentially expressed in HCT116 *p53*^{-/-} cells with or without serum starvation (Figure S3). p53 binding to these genes was also detected in HCT116 *p53*^{+/+} cells, and, therefore, these genes are also potential target genes of FL-p53. All these genes have previously been reported as p53 target genes by other groups.²⁵⁻²⁸ We previously established p53-null Saos2 cell lines that stably express a temperature-sensitive (ts) FL-p53 or a ts- $\Delta 1\text{stTAD-p53}$ by retrovirus-mediated gene transfer.¹² These ts mutants have the ability to bind to p53 binding sequences and transactivate its target genes under permissive temperature, but lose their abilities under non-permissive temperature. We have shown previously that these cells express comparable levels of ts-FL-p53 or ts- $\Delta 1\text{stTAD-p53}$, and ts-FL-p53 efficiently induces expression of representative p53 target genes following a temperature shift to the permissive temperature or temperature shift plus γ -ray irradiation.¹² We also established a control cell line transduced with empty retrovirus expressing only the drug resistance gene. We performed microarray expression analysis on RNA prepared from cells treated under each condition. As previously reported, we found that *PLK2* is induced in cells that express either FL-p53 or $\Delta 1\text{stTAD-p53}$ (Figure 2A).¹² As shown in Figure 2B,C, we found that *PTP4A1* and *RPS27L* were also induced in both cells. Induction of these genes was only seen under permissive temperature, showing that the induction is dependent on the DNA binding ability of $\Delta 1\text{stTAD-p53}$. To confirm these results, we ectopically expressed $\Delta 1\text{stTAD-p53}$ in p53-null H1299 cells (Figure 2D). All three genes were efficiently induced by $\Delta 1\text{stTAD-p53}$, confirming that these genes are, indeed, $\Delta 1\text{stTAD-p53}$ -inducible genes (Figure 2E-G).

3.4 | Endogenously expressed Δ 1stTAD induces *PLK2*, *PTP4A1* and *RPS27L*

We next analyzed whether endogenously expressed Δ 1stTAD-p53 regulates expression of *PLK2*, *PTP4A1* and/or *RPS27L*. For this purpose, we compared the expression of *PLK2*, *PTP4A1* and *RPS27L* mRNA in HCT116 *p53* +/+ and -/- cells. As shown in Figure 3A,B and Figure S3A-C, expression of *PLK2* and *PTP4A1* was higher in HCT116 *p53* -/- cells compared to HCT116 *p53* +/+ cells. This result presumably reflects the high expression level of Δ 1stTAD-p53 in HCT116 *p53* -/- cells under basal conditions (Figure 1D). In contrast, expression of *RPS27L* was similar in HCT116 *p53* +/+ and -/- cells, despite the fact that FL-p53 expression level is quite low in HCT116 *p53* +/+ cells under basal conditions, suggesting that *RPS27L* is more strongly induced by FL-p53 compared to Δ 1stTAD-p53 (Figures 1 and 3BC, Figure S3A,D). Upon serum deprivation, expression of *PLK2* and *PTP4A1* remained almost unchanged and *RPS27L* was slightly increased (Figure 3A-C and Figure S3A-S3D). These results suggest that although these three genes are Δ 1stTAD-p53-inducible genes, they are not equally regulated and some factors other than Δ 1stTAD-p53 may affect their expression. We next analyzed whether depletion of Δ 1stTAD-p53 in HCT116 *p53* -/- cells affects expression of *PLK2*, *PTP4A1* and/or *RPS27L*. As shown in Figure 3D-G, partial knock down of Δ 1stTAD-p53 resulted in decreased expression of *PLK2*, *PTP4A1* and *RPS27L*. These results demonstrate that endogenously expressed Δ 1stTAD-p53 induces *PLK2*, *PTP4A1* and *RPS27L*.

3.5 | *PLK2*, *PTP4A1* and *RPS27L* are p53 target genes that require the activity of the 2nd transactivation domain of p53

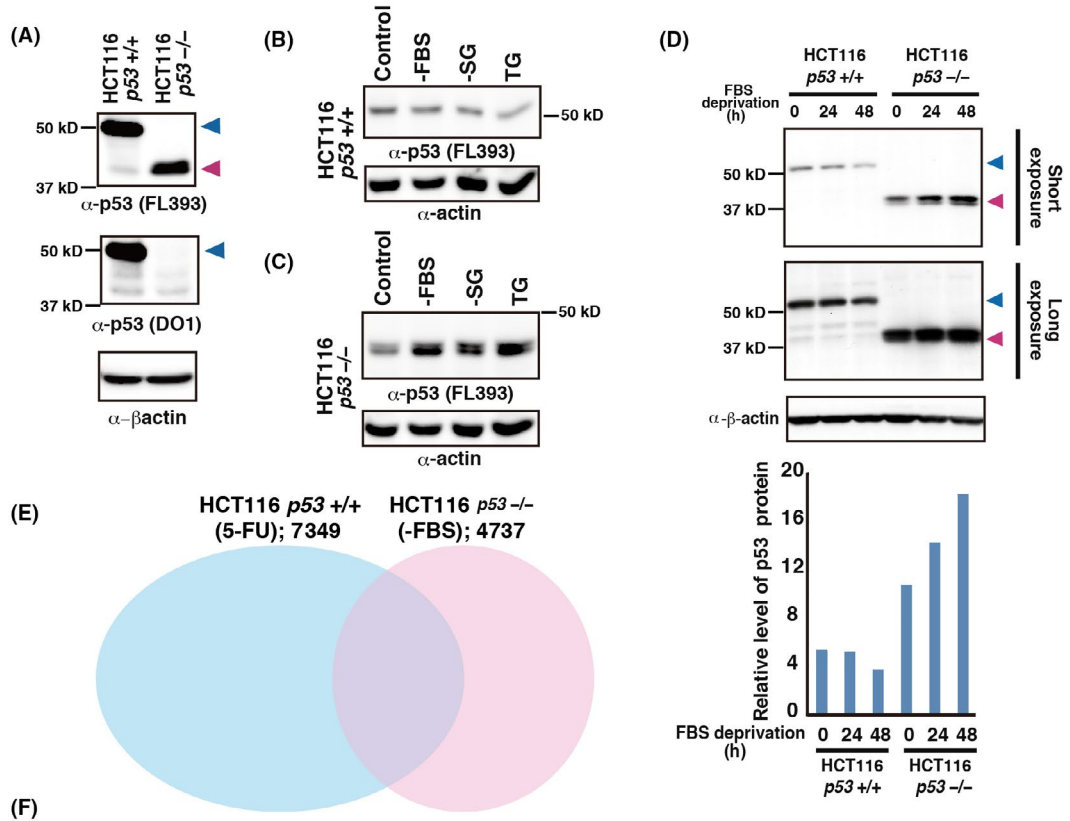
FL-p53 contains both the 1st and 2nd TAD of p53, while Δ 1stTAD-p53 contains only the 2nd TAD. Because *PLK2*, *PTP4A1* and *RPS27L* are induced by either FL-p53 or Δ 1stTAD-p53, we further examined the requirements for the 1st and the 2nd TAD of p53. For this purpose, we generated two additional mutant p53s: W53Q/F54S, which retains activity of the 1st TAD while the 2nd

TAD is inactive; and Δ 1stTAD-p53 W53Q/F54S, in which both TAD are inactive (Figure 4A-K). Expression of each p53 was confirmed by western blotting (Figure 4B,G). We observed that the 2nd TAD is required for full expression of previously reported p53 target gene *PHLDA3*, as have previously reported (Figure 4F,K).^{15,22} In addition, expression of *PLK2*, *PTP4A1* and *RPS27L* require the activity of the 2nd TAD of both FL-p53 and Δ 1stTAD-p53 (Figure 4C-E,H-J). These results show that *PLK2*, *PTP4A1* and *RPS27L* are inducible by either FL-p53 or Δ 1stTAD-p53, and this induction requires the activity of the 2nd TAD of p53.

3.6 | *PLK2*, *PTP4A1* and *RPS27L* are direct target genes of Δ 1stTAD-p53

We next used ChIP-seq and ChIP-chip analysis to examine whether *PLK2*, *PTP4A1* and *RPS27L* are direct target genes of FL-p53 and/or Δ 1stTAD-p53. We analyzed HCT116 *p53* -/- cells subjected to FBS deprivation and HCT116 *p53* +/+ cells either treated or not treated with 5-FU. As shown in Figure 5A-C, Figure S4 and Table S2, we observed binding of both FL-p53 and Δ 1stTAD-p53 to the *PLK2*, *PTP4A1* and *RPS27L* genomic regions in HCT116 *p53* +/+ or *p53* -/- cells. To further confirm the results, a ChIP assay was performed using p53-null Saos2 cells expressing temperature-sensitive FL-p53 or Δ 1stTAD-p53 (Figure 6A). Using these cells, binding of both FL-p53 and Δ 1stTAD-p53 to the *PLK2*, *PTP4A1* and *RPS27L* genomic regions was confirmed. p53 binding to the *PLK2* genomic region was observed at approximately 2 kb upstream of the transcription initiation site. We observed H3K27 acetylation within this region in 5-FU-treated HCT116 *p53* +/+ cells, indicating transcriptional activity induced by 5-FU. We also detected H3K4 tri-methylation surrounded by H3K4 mono-methylation at the *PLK2* gene promoter region, indicating that *PLK2* is actively transcribed in both unstressed and stressed conditions. In contrast, p53 binding was observed within intron 1 of both the *PTP4A1* and *RPS27L* genomic regions, and these regions were positive for H3K27 acetylation in HCT116 *p53* +/+ cells regardless of 5-FU treatment, although acetylation increased upon 5-FU treatment. This indicates that these regions are transcriptionally active even in the basal condition, and further induced upon 5-FU treatment. We also detected

FIGURE 1 Comprehensive analysis of Δ 1stTAD-p53 binding sites. A-D, Western blotting was performed using anti-p53 polyclonal antibody (FL393; A upper panel and B-D) or monoclonal antibody (DO1; A lower panel). Blots with anti- β -actin confirmed equal protein loading in each lane. Blue and red arrowheads denote FL-p53 and Δ 1stTAD-p53, respectively. A, Lysates were from HCT116 *p53* +/+ cells treated with fluorouracil (5-FU) for 16 h or HCT116 *p53* -/- cells cultured under basal conditions. B, C, HCT116 *p53* +/+ (B) and -/- (C) cells were subjected to serum deprivation (-FBS, treated with 0.1% FBS, 48 h), Ser and Gly starvation (-SG, treated for 24 h) or thapsigargin treatment (TG, treated with 500 nmol/L, 18 h). D, The levels of p53 proteins were quantified and are shown as a graph at the bottom. E, FL-p53 and Δ 1stTAD-p53 binding sites were analyzed by ChIP-seq analysis, and the results are summarized in a Venn diagram. HCT116 *p53* +/+ cells treated with 5-FU and serum deprived HCT116 *p53* -/- cells were used for ChIP-seq analysis. F-H, Analysis of FL-p53 and Δ 1stTAD-p53 binding sequences using HOMER software. Motif analyses were carried out using p53 binding sites selected in E. Binding sites found in both HCT116 *p53* +/+ and -/- cells (F), only in HCT116 *p53* +/+ cells (G) and sites only found in HCT116 *p53* -/- cells (H) were analyzed. Motifs with significant *P*-values (<1E-100) are shown. I, Numbers of potential target genes of Δ 1stTAD-p53. Expression of genes selected in E was analyzed, and genes with significant change in expression levels between the samples (*P*-values less than 0.05) were selected. Numbers of selected genes with binding sites common for FL-p53 and Δ 1stTAD-p53 and genes with specific binding of Δ 1stTAD-p53 are shown



Rank	Motif	P-value	% of targets	% of BG	Best match/details
1		1.E-2232	52.45	0.15	p53(p53)/Saos-p53-ChIP-Seq(GSE15780)/Homer(0.958)
2		1.E-244	4.47	0.00	GATA6/MA1104.1/Jaspar(0.677)
3		1.E-156	3.04	0.00	STAT5(Stat)/mCD4+-Stat5-ChIP-Seq(GSE12346)/Homer(0.688)
4		1.E-153	3.30	0.00	PB0078.1_Srf_1/Jaspar(0.712)
5		1.E-148	3.41	0.01	TEAD2(TEA)/Py2T-Tead2-ChIP-Seq(GSE55709)/Homer(0.567)
6		1.E-148	3.19	0.01	TFAP2C(var.2)/MA0814.1/Jaspar(0.595)
7		1.E-147	2.88	0.00	PH0114.1_Nkx2-5/Jaspar(0.551)
8		1.E-145	3.14	0.00	NFAT(RHD)/Jurkat-NFATC1-ChIP-Seq(Jolma_et_al)/Homer(0.686)
9		1.E-134	2.66	0.00	VDR/MA0693.2/Jaspar(0.524)
10		1.E-131	2.61	0.00	ZNF415(Z1)/HEK293-ZNF415.GFP-ChIP-Seq(GSE58341)/Homer(0.576)
11		1.E-125	2.50	0.00	Foxf1(Forkhead)/Lung-Foxf1-ChIP-Seq(GSE77951)/Homer(0.640)
12		1.E-119	2.66	0.01	CHR/Hela-CellCycle-Expression/Homer(0.576)
13		1.E-116	2.34	0.00	PB0012.1_EIK3_1/Jaspar(0.605)
14		1.E-111	2.50	0.01	Sox4(HMG)/proB-Sox4-ChIP-Seq(GSE50068)/Homer(0.650)
15		1.E-109	2.88	0.01	NRF1(NRF)/MCF7-NRF1-ChIP-Seq(Unpublished)/Homer(0.532)
16		1.E-105	2.40	0.01	PB0060.1_Smad3_1/Jaspar(0.583)
17		1.E-103	2.13	0.00	EBF1/MA0154.3/Jaspar(0.609)

(G)

Rank	Motif	P-value	% of targets	% of BG	Best match/details
1		1.E-5825	62.56	0.80	p53(p53)/Saos-p53-ChIP-Seq(GSE15780)/Homer(0.985)
2		1.E-175	1.48	0.01	Gata1(Zf)/K562-GATA1-ChIP-Seq(GSE18829)/Homer(0.640)
3		1.E-158	1.22	0.00	Twist2(MA0633.1)/Jaspar(0.576)
4		1.E-148	1.14	0.00	PB0078.1_Srf_1/Jaspar(0.717)
5		1.E-126	1.00	0.00	NFAT5(MA0606.1)/Jaspar(0.596)
6		1.E-113	0.92	0.00	Foxo3(Forkhead)/U2OS-Foxo3-ChIP-Seq(E-MTAB-2701)/Homer(0.580)
7		1.E-104	0.97	0.01	ONECUT3(MA0757.1)/Jaspar(0.624)

(H)

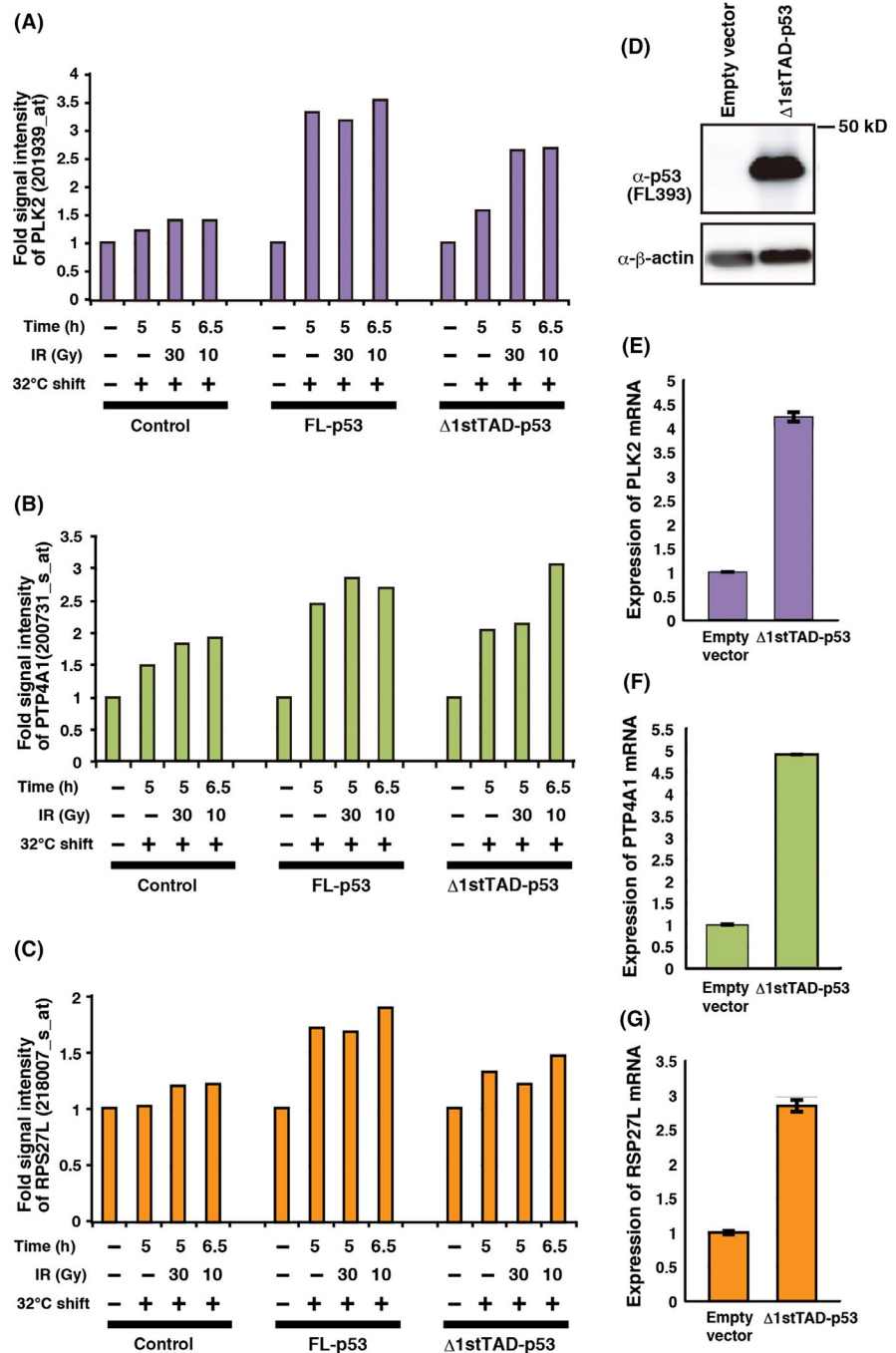
Rank	Motif	P-value	% of targets	% of BG	Best match/details
1		1E-313	5.64	0.03	STAT5(Stat)/mCD4+-Stat5-ChIP-Seq(GSE12346)/Homer(0.681)
2		1E-300	6.13	0.05	CHR/Hela-CellCycle-Expression/Homer(0.592)
3		1E-290	5.85	0.04	MTF1(MA0863.1)/Jaspar(0.557)
4		1E-284	5.51	0.04	PH0111.1_Nkx2-2/Jaspar(0.590)
5		1E-282	5.33	0.03	PB0116.1_Elf3_2/Jaspar(0.600)
6		1E-251	4.47	0.02	Sox1(MA0870.1)/Jaspar(0.576)
7		1E-240	4.92	0.04	RXRA::VDR(MA0074.1)/Jaspar(0.500)
8		1E-198	3.60	0.02	IRF1(IRF)/PBMC-IRF1-ChIP-Seq(GSE43036)/Homer(0.571)
9		1E-197	4.16	0.04	STAT1::STAT2(MA0517.1)/Jaspar(0.634)
10		1E-188	3.91	0.03	BMXB(HTH)/Hela-BMYB-ChIP-Seq(GSE27030)/Homer(0.550)
11		1E-165	3.36	0.03	PBX1(MA0070.1)/Jaspar(0.594)
12		1E-133	2.74	0.02	Tcf3(HMG)/mES-Tcf3-ChIP-Seq(GSE11724)/Homer(0.539)
13		1E-108	2.22	0.02	NFATC2(MA0152.1)/Jaspar(0.582)

(I)

Binding sites	mRNA level	Number of genes
Common for FL-p53 and Δ1stTAD-p53	Up	62
	Down	40
Δ1stTAD-p53 only	Up	87
	Down	63

FIGURE 1 continued

FIGURE 2 *PLK2*, *PTP4A1* and *RPS27L* are $\Delta 1stTAD$ -p53-inducible genes. A-C, Expression of *PLK2* (A), *PTP4A1* (B) and *RPS27L* (C) was analyzed by microarray expression analysis. Temperature-sensitive wild-type-expressing, $\Delta 1stTAD$ -p53-expressing or control Saos2 cells were tested for induction of *PLK2*, *PTP4A1* and *RPS27L* upon temperature shift to the permissive temperature with or without γ -ray irradiation. Cells were subjected to γ -ray irradiation (30 or 10 Gy) 2 h after temperature shift to 32°C. Cells were collected 5 or 6.5 h post-temperature shift. Relative induction of the genes in three cell lines upon temperature shift is shown. D-G, H1299 cells were infected with adenoviruses expressing control Lac Z or $\Delta 1stTAD$ -p53 at MOI (multiplicity of infection) 6, and harvested 48 h post-infection. Expression of $\Delta 1stTAD$ -p53 was analyzed by western blotting (D). *PLK2* (E), *PTP4A1* (F) and *RPS27L* (G) mRNA levels were analyzed by quantitative RT-PCR.



H3K4 tri-methylation surrounded by H3K4 mono-methylation at the *PTP4A1* and *RPS27L* gene promoter regions, indicating that they are actively transcribed in both unstressed and stressed conditions. We also found sequences highly similar to the p53 consensus binding sequences within the p53 binding regions of each gene (Figure 6B). These three genes have previously been identified as p53 target genes,²⁵⁻²⁸ and the p53 binding sequences we identified were the same as previously described for *PLK2* and *PTP4A1*, but different for *RPS27L*. The p53 binding sequence in *RPS27L* was previously reported to be 5'-GGGCATGTagtGACTTGCCC-3' (chr15: 61236487-61236506, NCBI36/hg18; sequences shown in upper case match the consensus

p53 binding sequence).^{27,28} This sequence overlapped the p53 binding sequence that we identified (chr15: 61236477-61236496). The calculated TRANSFAC match score for the sequence we identified is 0.704, while the score for the previously reported sequence is 0.621.

To further analyze whether the p53 binding sequences are bound and activated by p53, the genomic region containing the sequences were cloned and assayed for $\Delta 1stTAD$ -p53 responsiveness by luciferase reporter assay. As shown in Figure 6C-E, $\Delta 1stTAD$ -p53 responsiveness was detected for all three reporter genes. These data collectively show that *PLK2*, *PTP4A1* and *RPS27L* are direct target genes of both FL-p53 and $\Delta 1stTAD$ -p53.

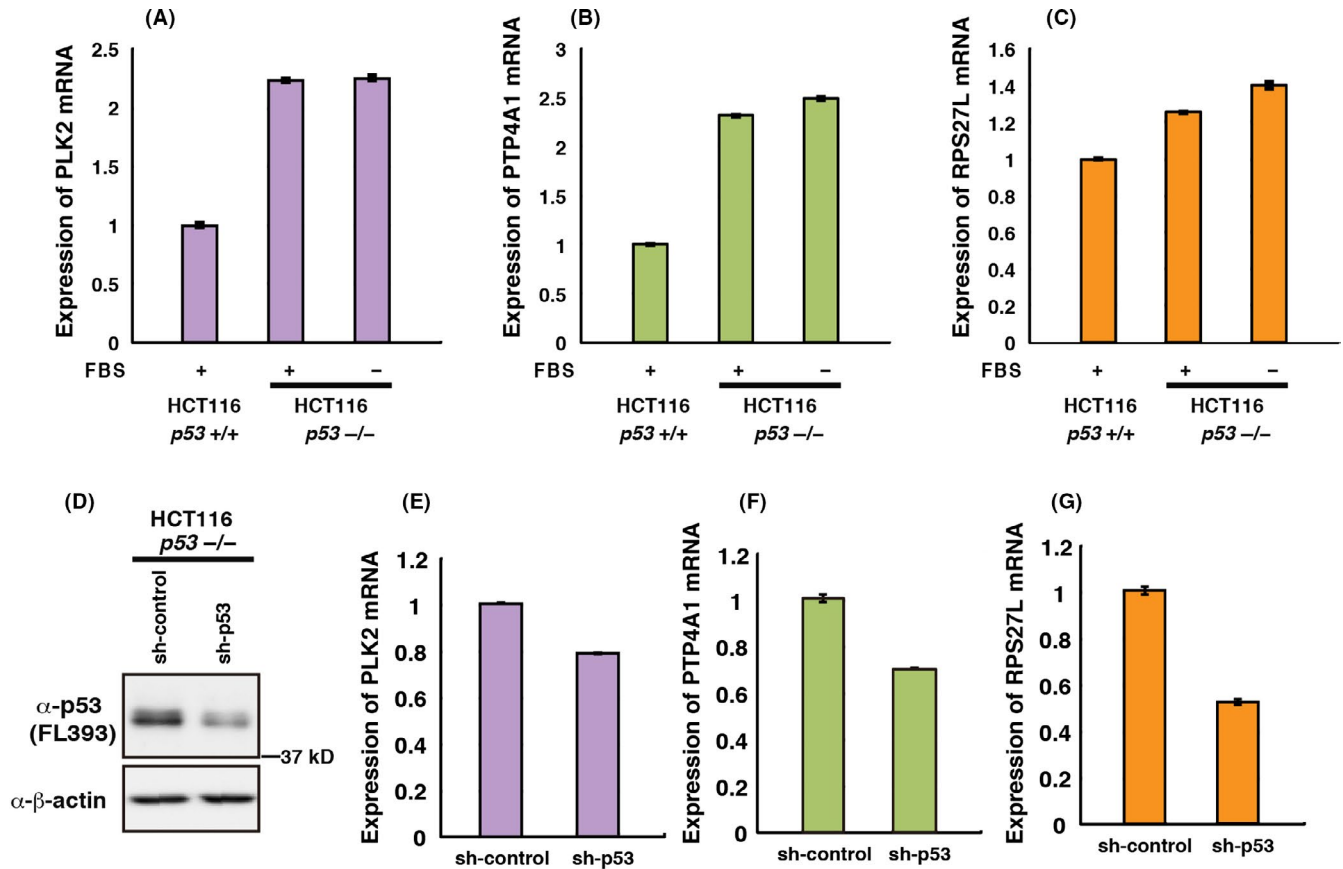


FIGURE 3 Endogenous $\Delta 1$ stTAD-p53 induces *PLK2*, *PTP4A1* and *RPS27L*. A-C, Expression of *PLK2* (A), *PTP4A1* (B) and *RPS27L* (C) were analyzed by quantitative RT-PCR in HCT 116 *p53* +/+ and -/- cells. HCT116 *p53* -/- cells were cultured in normal FBS or subjected to FBS deprivation for 42 h. (D-G), Control shRNA or shRNA against p53 were stably introduced into HCT116 *p53* -/- cells. p53 protein expression levels were analyzed by western blotting (D). *PLK2* (E), *PTP4A1* (F) and *RPS27L* (G) mRNA levels were analyzed by quantitative RT-PCR

3.7 | *PLK2* and *PTP4A1* are induced upon endoplasmic reticulum stress

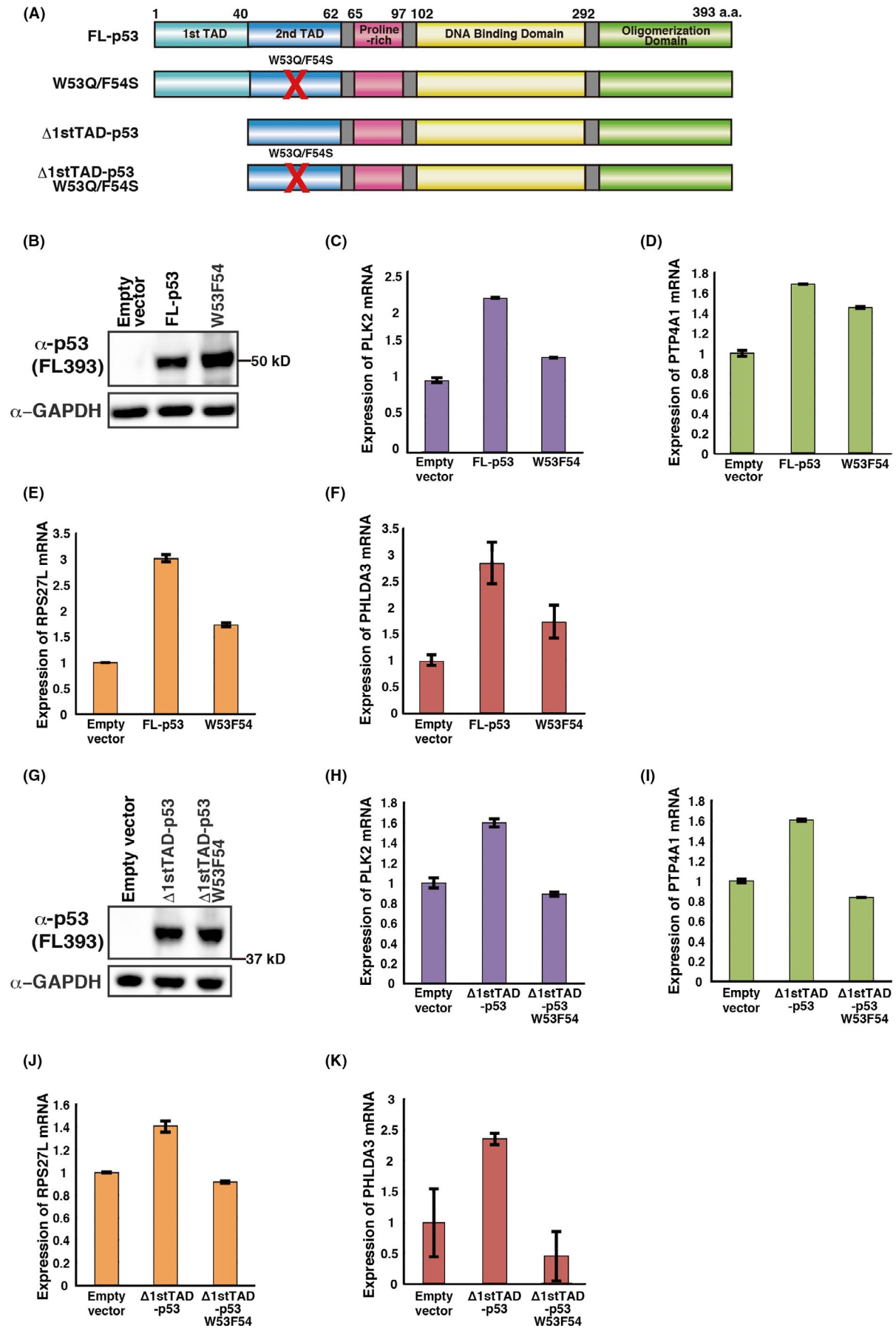
As shown in Figure 1C, $\Delta 1$ stTAD-p53 expression was elevated upon ER stress induced by TG treatment. We therefore analyzed whether *PLK2*, *PTP4A1* and *RPS27L* are induced upon ER stress (Figure 7A-I). We first analyzed the time course of $\Delta 1$ stTAD-p53 upregulation upon TG treatment. As shown in Figure 7A,B, expression of FL-p53 decreased upon TG treatment, while that of $\Delta 1$ stTAD-p53 increased. Interestingly, upon TG treatment, $\Delta 1$ stTAD-p53 was phosphorylated at Ser46, a residue reported to be involved in the enhancement of the apoptosis-inducing ability of p53.^{29,30} This suggests the possibility that TG treatment leads to Ser46-induced activation of $\Delta 1$ stTAD-p53 (Figure 7C). We next analyzed the mRNA expression levels of *PLK2*, *PTP4A1* and *RPS27L*. As shown in Figure 7D,E, *PLK2* and *PTP4A1* expression were increased upon TG treatment in both HCT116 *p53* +/+ and -/- cells but were increased higher in HCT116 *p53* -/- cells. In contrast, expression of *RPS27L* was not changed significantly upon TG treatment in either

HCT116 *p53* +/+ or -/- cells (Figure S5). We therefore focused on *PLK2* and *PTP4A1*, and further analyzed whether expression of these genes in HCT116 *p53* -/- cells is dependent on $\Delta 1$ stTAD-p53. We knocked down $\Delta 1$ stTAD-p53, and as shown in Figure 7F,I, $\Delta 1$ stTAD-p53 expression was effectively knocked down by siRNA against p53. Both basal and TG-induced *PTP4A1* expression were decreased by $\Delta 1$ stTAD-p53 knock down (Figure 7G). Basal *PLK2* expression was also decreased by $\Delta 1$ stTAD-p53 knock down, but TG-induced *PLK2* expression was not significantly affected (Figure 7H). Thus, while TG-induced *PTP4A1* expression in HCT116 *p53* -/- cells is dependent on $\Delta 1$ stTAD-p53, TG-induced *PLK2* expression is not dependent on $\Delta 1$ stTAD-p53.

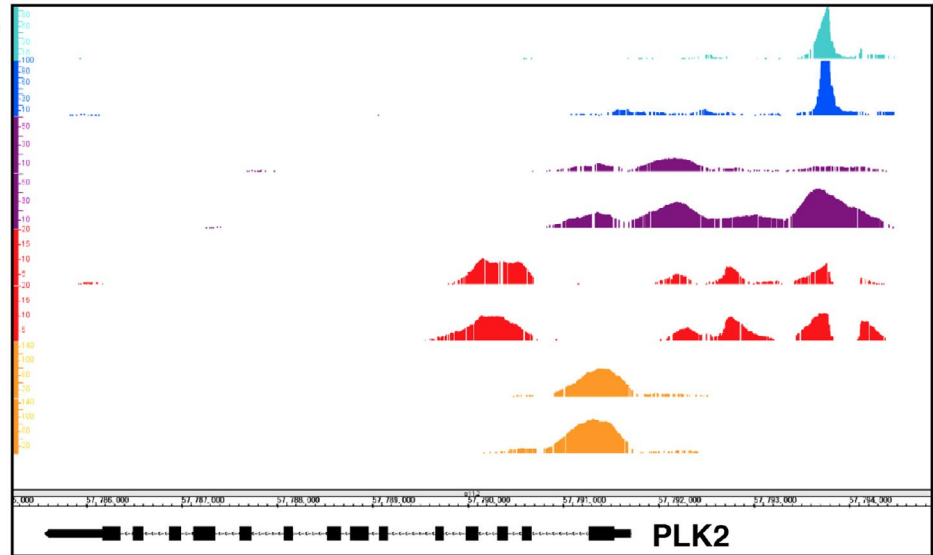
3.8 | *PTP4A1* suppresses endoplasmic reticulum stress-dependent apoptosis

Because we found that *PTP4A1* is induced by TG treatment, we next analyzed the function of *PTP4A1* upon ER stress. We knocked down

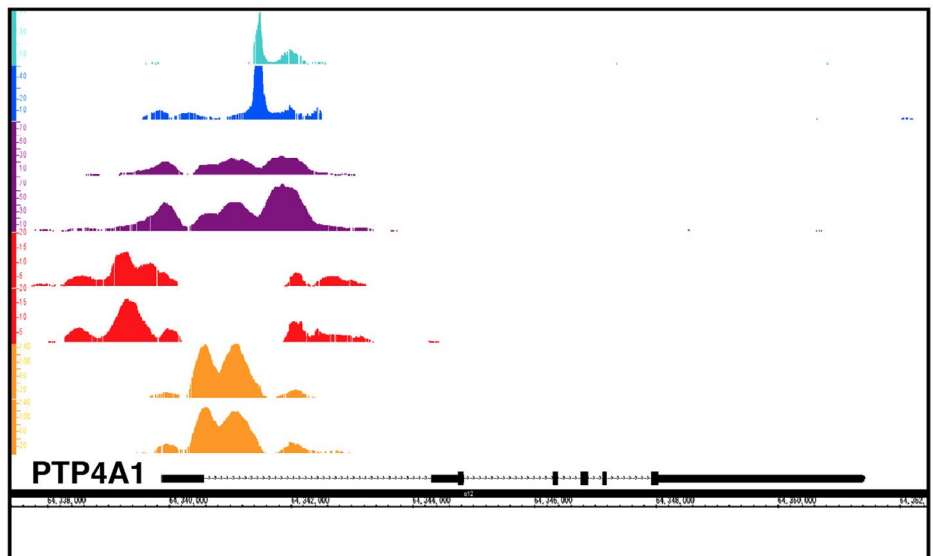
FIGURE 4 Transcription of *PLK2*, *PTP4A1* and *RPS27L* are induced in a manner dependent on the activity of the 2nd transactivation domain of p53. A, Schema of p53 constructs used in this study. B, G, Expression of p53 constructs was analyzed by western blotting. (C-F, H-K), H1299 cells were transfected with the indicated p53 constructs and harvested 24 h post-transfection. *PLK2* (C, H), *PTP4A1* (D, I), *RPS27L* (E, J) and *PHLDA3* (F, K) mRNA levels were analyzed by quantitative RT-PCR



- (A) p53 HCT116 *p53*^{-/-} FBS
 p53 HCT116 *p53*^{+/+} 5-FU
 K27ac HCT116 *p53*^{+/+} NT
 K27ac HCT116 *p53*^{+/+} 5-FU
 K4me1 HCT116 *p53*^{+/+} NT
 K4me1 HCT116 *p53*^{+/+} 5-FU
 K4me3 HCT116 *p53*^{+/+} NT
 K4me3 HCT116 *p53*^{+/+} 5-FU



- (B) p53 HCT116 *p53*^{-/-} FBS
 p53 HCT116 *p53*^{+/+} 5-FU
 K27ac HCT116 *p53*^{+/+} NT
 K27ac HCT116 *p53*^{+/+} 5-FU
 K4me1 HCT116 *p53*^{+/+} NT
 K4me1 HCT116 *p53*^{+/+} 5-FU
 K4me3 HCT116 *p53*^{+/+} NT
 K4me3 HCT116 *p53*^{+/+} 5-FU



- (C) p53 HCT116 *p53*^{-/-} FBS
 p53 HCT116 *p53*^{+/+} 5-FU
 K27ac HCT116 *p53*^{+/+} NT
 K27ac HCT116 *p53*^{+/+} 5-FU
 K4me1 HCT116 *p53*^{+/+} NT
 K4me1 HCT116 *p53*^{+/+} 5-FU
 K4me3 HCT116 *p53*^{+/+} NT
 K4me3 HCT116 *p53*^{+/+} 5-FU

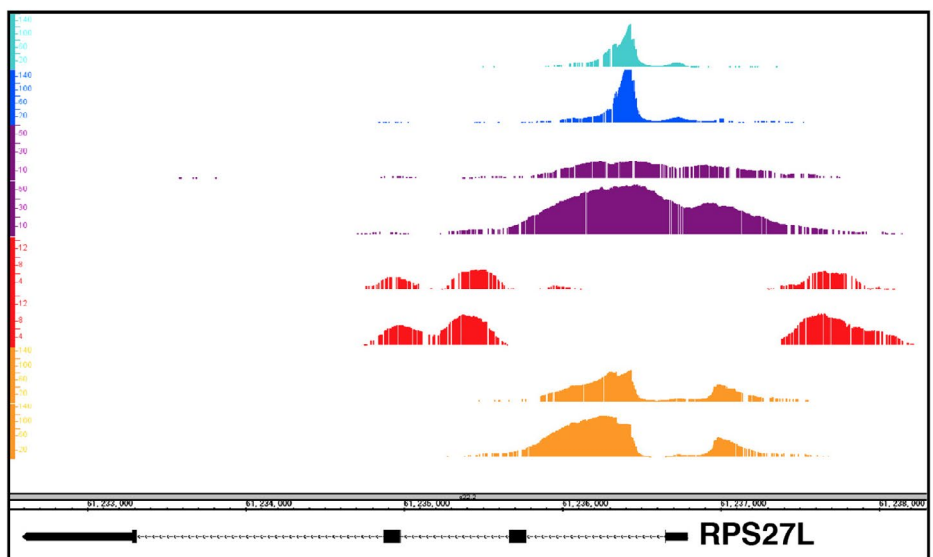


FIGURE 5 *PLK2*, *PTP4A1* and *RPS27L* are direct target genes of both FL-p53 and $\Delta 1\text{stTAD-p53}$. A-C, Genomic loci of *PLK2* (chr5:57,783,671-57,798,263) (A), *PTP4A1* (chr6:64,332,522-64,369,290) (B) and *RPS27L* (chr15:61,232,500-61,238,300) (C) are shown together with the ChIP-seq results. HCT116 *p53*^{+/+} cells treated with or without fluorouracil (5-FU) and serum-deprived HCT116 *p53*^{-/-} cells were used for ChIP-seq analysis. ChIP-seq analyses were performed using antibodies against p53, H3K27ac, H3K4me1 and H3K4me3. The resulting sequences were mapped to the build #36 reference human genome (hg18)

PTP4A1 by siRNA and analyzed the DNA content of the cells by FACS (Figure 8A,B). We found that compared to control siRNA-treated cells, *PTP4A1* siRNA-treated cells had higher sub-G1 DNA content upon TG treatment (Figure 8B). In addition, as shown in Figure 8A,C, these cells also had higher levels of cleaved PARP and cleaved caspase 3, and contained a higher number of TUNEL-positive cells compared to control cells. Next, we ectopically expressed *PTP4A1* by adenovirus-mediated gene transfer. As shown in Figure 8D,E, overexpression of *PTP4A1* resulted in a decrease in the fraction of cells exhibiting sub-G1 DNA content induced by TG treatment. Finally, we analyzed the subcellular localization of *PTP4A1* following TG treatment. As shown in Figure 8F, under basal conditions *PTP4A1* was localized to the cytoplasmic region, except for the ER, and accumulated in the ER region following TG treatment. These results collectively indicate that *PTP4A1* suppresses TG-induced apoptosis by upregulating the unfolded protein response and relocates to the ER in response to ER stress, where it potentially exerts some specific function.

3.9 | *PLK2* induces endoplasmic reticulum stress-dependent apoptosis

Although upregulation of *PLK2* upon ER stress is not $\Delta 1\text{stTAD-p53}$ -dependent, the function of *PLK2* in ER stress has not been clarified. Because we found that *PLK2* is also induced by TG treatment, we next analyzed its function in ER stress (Figure 9A-G). We knocked down *PLK2* by siRNA and analyzed the DNA content of the cells by FACS (Figure 9A,C). Compared to control siRNA-treated cells, *PLK2* siRNA-treated cells had lower sub-G1 DNA content (Figure 9C). Furthermore, we observed fewer TUNEL-positive cells in the *PLK2* knocked down cells compared to control cells, as well as less cleaved PARP and cleaved caspase 3 expression (Figure 9B,D). We next ectopically expressed *PLK2* by adenovirus-mediated gene transfer. As shown in Figure 9E,F, expression of *PLK2* had no effect on TG-induced apoptosis, suggesting the possibility that endogenously

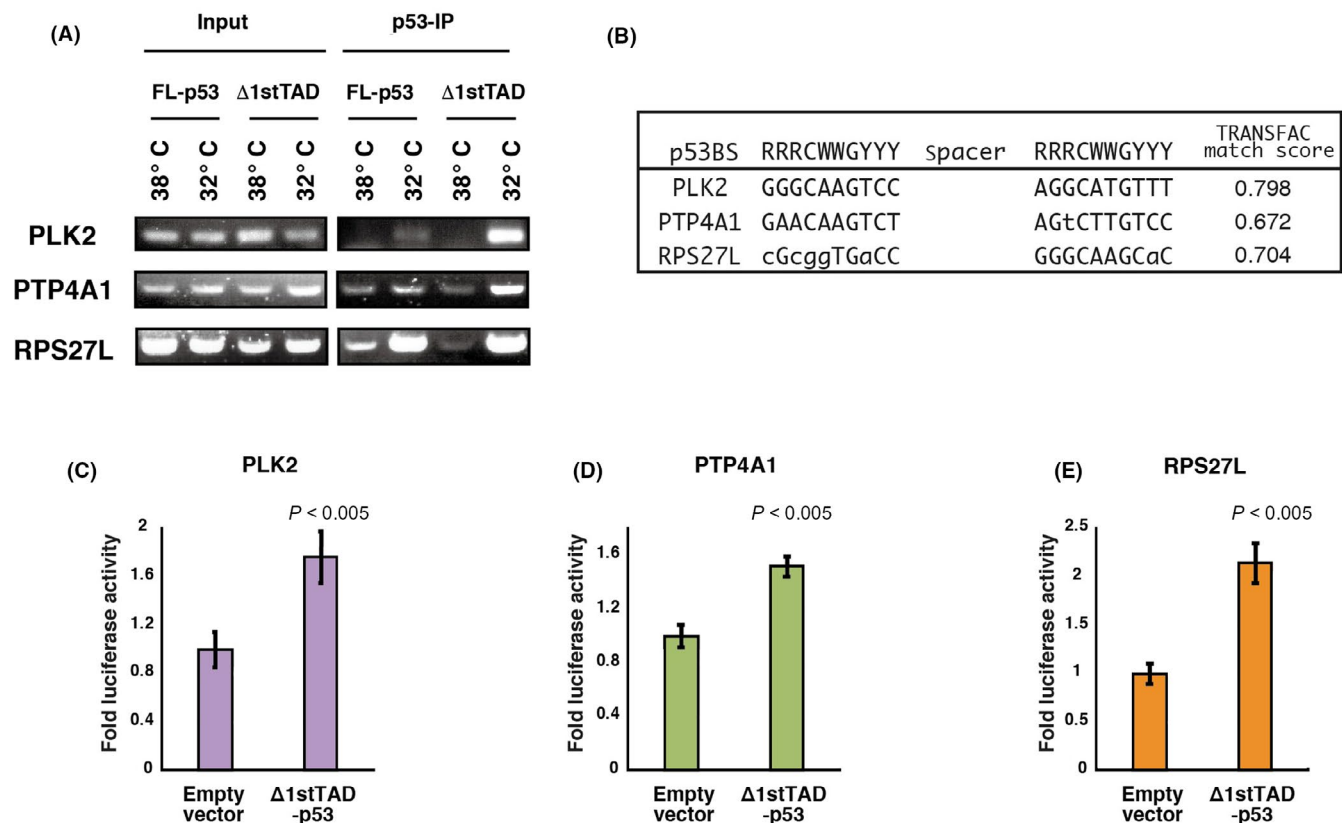


FIGURE 6 The p53 responsive elements of *PLK2*, *PTP4A1* and *RPS27L* are bound and activated by $\Delta 1\text{stTAD-p53}$. A, ChIP assay was performed for the *PLK2*, *PTP4A1* and *RPS27L* promoters. Saos2 cell lines expressing ts-FL-p53 or ts- $\Delta 1\text{stTAD-p53}$ were used to analyze p53 binding to the promoters upon temperature shift to the permissive temperature. B, Nucleotide sequences of p53 binding sites together with the consensus p53 binding sequences are shown. Sequences that match the consensus sequences are shown in upper case. TRANSFAC match scores are also calculated. C-E, The p53 binding sequences of *PLK2* (C), *PTP4A1* (D) and *RPS27L* (E) were cloned upstream of firefly luciferase reporter gene with a minimal promoter, and a luciferase reporter assay was performed. The experiment was run in triplicate, and data are represented as the mean fold activation \pm SD

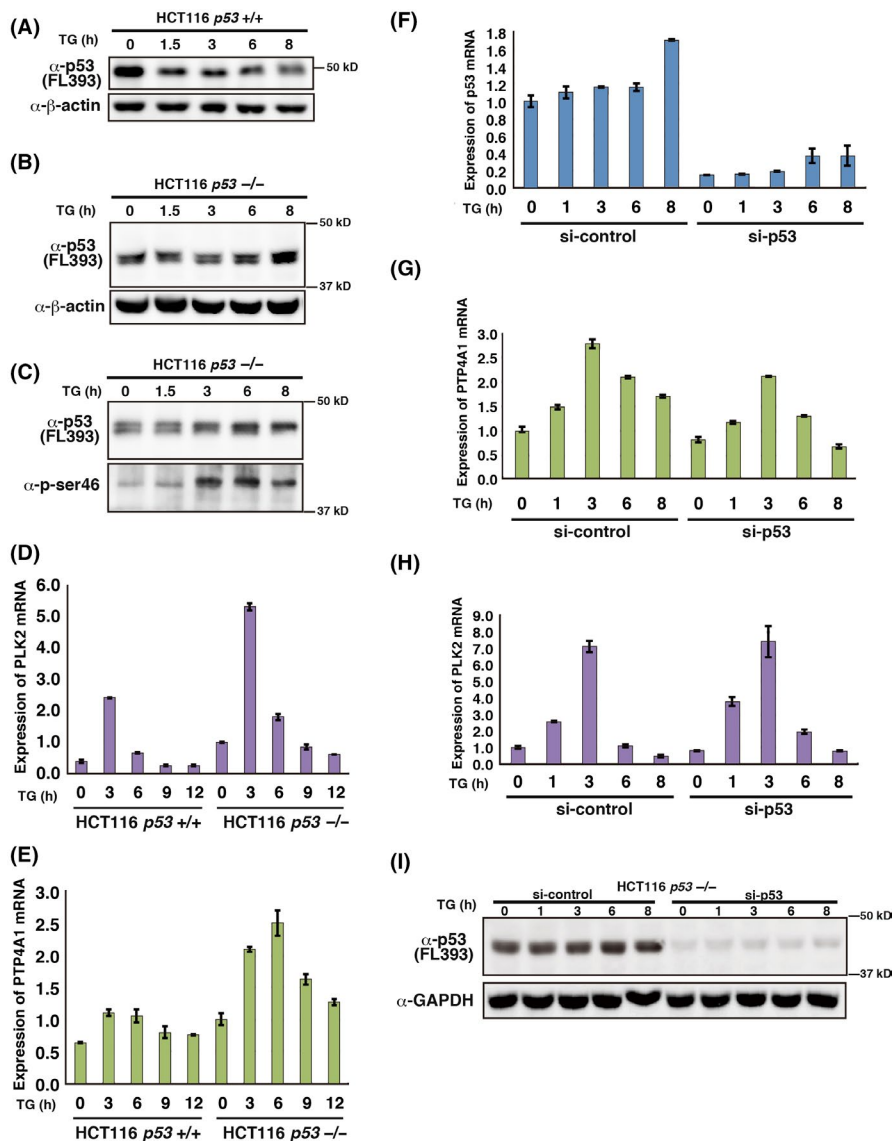


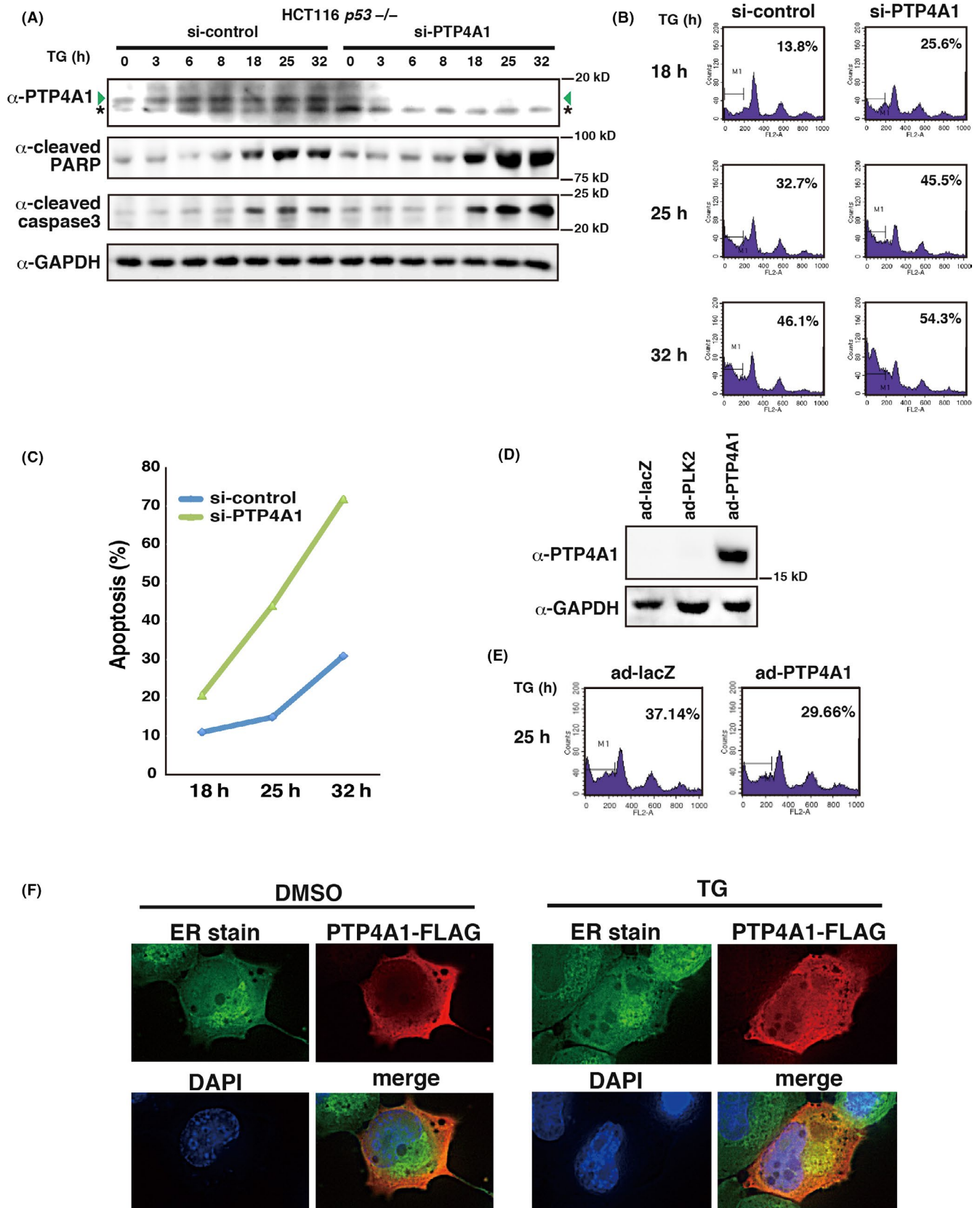
FIGURE 7 *PLK2* and *PTP4A1* are induced upon ER stress. A-E, HCT 116 *p53*^{+/+} and *p53*^{-/-} cells were treated with 500 nmol/L thapsigargin (TG). Cells were harvested at the indicated times post-treatment. p53 and β -actin protein expression levels were analyzed by western blotting (A, B). p53 phospho-Ser 46 protein levels were analyzed from immunoprecipitated p53 (C). Immunoprecipitation of p53 was performed using anti-p53 antibodies (Pab421 and Pab1801). *PLK2* (D) and *PTP4A1* (E) mRNA levels were analyzed by quantitative RT-PCR. F-I, HCT 116 *p53*^{-/-} cells were transfected with control siRNA or siRNA against *p53*. Cells were treated with 500 nmol/L TG 40 h post-siRNA transfection and were harvested at the indicated times post-TG treatment. Expression of *p53* (F), *PTP4A1* (G) and *PLK2* (H) mRNA levels was analyzed by quantitative RT-PCR. Expression of p53 and GAPDH protein levels were analyzed by western blotting (I)

expressed *PLK2* is sufficient to induce apoptosis upon TG treatment. Finally, we analyzed the subcellular localization of *PLK2* with or without TG treatment. As shown in Figure 9G, *PLK2* localized to the cytoplasmic region overlapping the ER region under basal conditions but translocated to the plasma membrane upon TG treatment. These results collectively indicate that *PLK2* enhances TG-induced apoptosis and may have a function at the plasma membrane in response to ER stress.

4 | DISCUSSION

Recently, several reports have confirmed the relevance of the 2nd TAD within *p53* in the induction of tumor suppression, apoptosis and senescence.^{7,12-18,31} Therefore, understanding how *p53* modulates these biological functions requires a better characterization of the function of the 2nd TAD. The Δ 1stTAD-*p53* construct, which retains only the 2nd TAD, is an ideal *p53* variant for studying the

FIGURE 8 *PTP4A1* suppresses endoplasmic reticulum (ER) stress-dependent cell death. A-C, HCT 116 *p53*^{-/-} cells were transfected with control siRNA or siRNA against *PTP4A1*. Cells were treated with 500 nmol/L TG 40 h post-siRNA transfection and were harvested at the indicated times post-TG treatment. A, Expression levels of *PTP4A1*, PARP, cleaved caspase 3 and GAPDH proteins were analyzed by western blotting. Green arrowhead and asterisk denote *PTP4A1* and non-specific bands, respectively. B, C, Cells with sub-G1 DNA content (B) and TUNEL-positive cells (C) were analyzed by FACS at the indicated times. The experiment was repeated three times and the representative data are shown (C). D, E, *PTP4A1* overexpression leads to suppression of ER stress-dependent cell death. HCT116 *p53*^{-/-} cells were infected with adenoviruses expressing control Lac Z (ad-lacZ) or *PTP4A1* (ad-*PTP4A1*) at 5 moi, treated with 500 nmol/L TG 24 h post-infection, and harvested 25 h post-TG treatment. Expression levels of *PTP4A1* protein were analyzed by western blotting (D). Cells with sub-G1 DNA content were analyzed by FACS (E). F, *PTP4A1* translocates to the ER under ER-stressed condition. H1299 cells were transfected with control or *PTP4A1*-FLAG expression vectors, and cells were treated with control DMSO or 500 nmol/L thapsigargin for 6 h. Localization of *PTP4A1*-FLAG was visualized by anti-FLAG antibody. ER was detected by ER stain



function of the 2nd TAD of p53. In this study, we identified a number of Δ 1stTAD-p53-inducible genes by microarray expression and ChIP-seq analysis, and comprehensively analyzed the sequences of their Δ 1stTAD-p53 binding sites. We found that while some of

the Δ 1stTAD-p53 binding regions are shared with FL-p53, some of them are specific for Δ 1stTAD-p53. The binding sites shared with FL-p53 showed a high similarity to the p53 consensus binding sequences, whereas the sites specific for Δ 1stTAD-p53 were highly

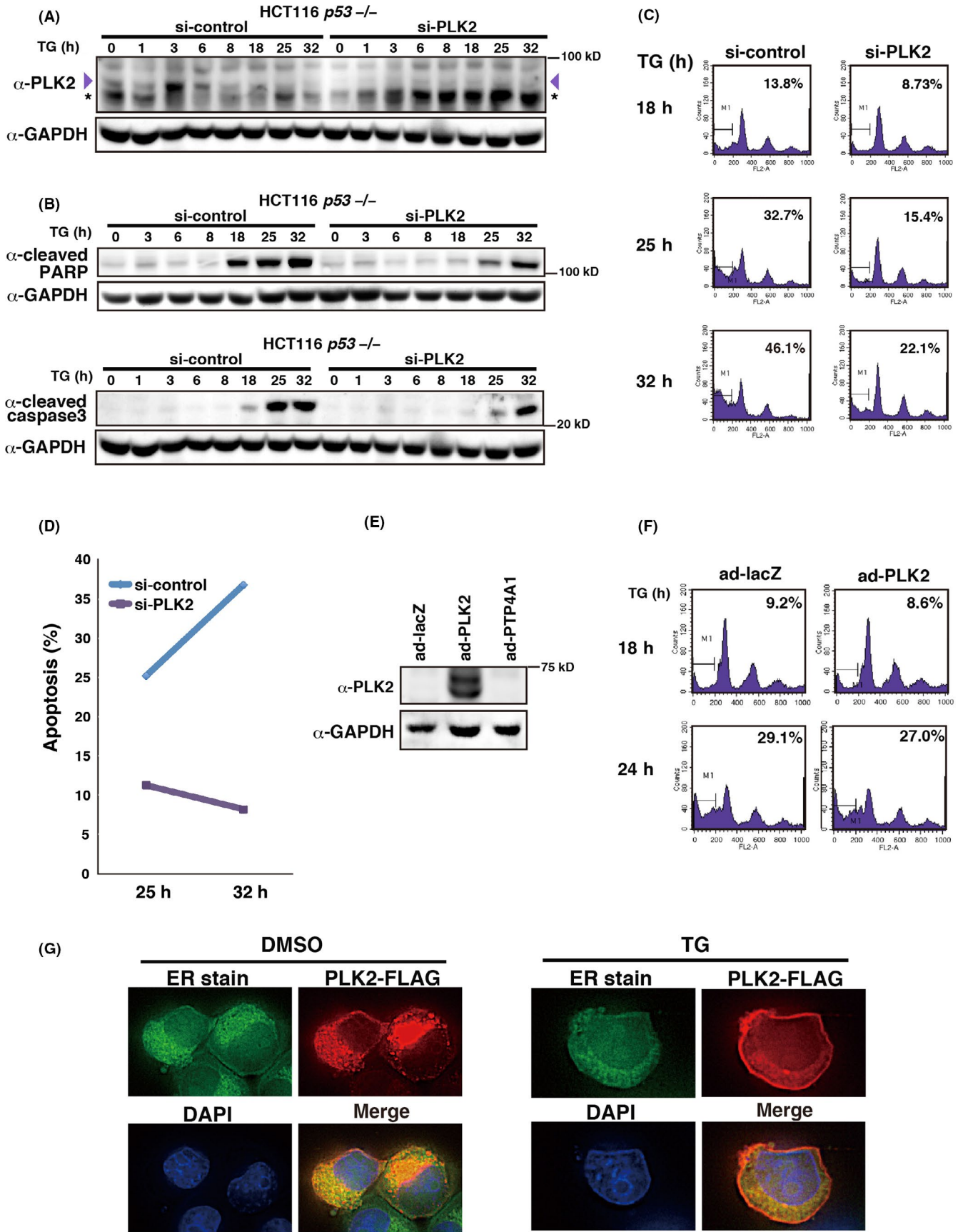


FIGURE 9 Knockdown of PLK2 suppresses endoplasmic reticulum (ER) stress-dependent cell death. A–D, HCT 116 p53 $-/-$ cells were transfected with control siRNA or siRNA against *PLK2*, and were analyzed as in Figure 8A–C. A, B, Expression of *PLK2*, *PARP*, cleaved caspase 3 and *GAPDH* protein levels were analyzed by western blotting. Purple arrowhead and asterisk denote *PLK2* and non-specific bands, respectively. C, D, Cells with sub-G1 DNA content (C) and TUNEL-positive cells (D) were analyzed by FACS. E, F, *PLK2* overexpression does not enhance ER stress-dependent cell death. Adenoviruses expressing *PLK2* (ad-*PLK2*) were used and analyzed as in Figure 8D,E. Expression of *PLK2* protein levels was analyzed by western blotting (E). Cells with sub-G1 DNA content were analyzed by FACS (F). G, *PLK2* translocates to the plasma membrane under ER-stressed conditions. H1299 cells were transfected with control or *PLK2*-FLAG expression vectors and were analyzed as in Figure 8F

divergent and included sites with similarity to the binding sites for several other transcription factors. $\Delta 1stTAD$ -p53 may bind to these divergent sequences directly or indirectly, because p53 can localize to promoter regions through binding to other transcriptional factors (eg, *GATA-1* or *STAT-1*).^{32,33}

Furthermore, by combining the ChIP-seq data and microarray expression analysis data, we identified potential $\Delta 1stTAD$ -p53 target genes, among which there were three novel $\Delta 1stTAD$ -p53-induced target genes: *PLK2*, *PTP4A1* and *RPS27L*. Interestingly, two of these genes, *PLK2* and *PTP4A1*, are strongly induced upon ER stress and function to enhance and repress ER stress-induced apoptosis, respectively. Because ablation of *PTP4A1* results in enhancement of apoptosis upon ER stress, *PTP4A1* may protect cells from stresses. *PTP4A1* is a protein tyrosine phosphatase that promotes the growth and migration of tumor cells through unknown mechanisms.^{34,35} *PTP4A1* has very low activity in vitro and robust substrates have not been reported and some of the functions of *PTP4A1* are probably exerted through protein-protein interaction that does not require the phosphatase activity.^{36,37} Because *PTP4A1* localizes to ER upon ER stress, *PTP4A1* may act on some protein localized to ER. The precise molecular function of *PTP4A1* in ER stress warrants further investigation. In contrast, *PLK2* may function to induce apoptosis when cells are severely damaged by various types of stress. Previously, *PLK2* has been reported to be a p53 target gene that confers resistance to antimicrotubule agents.²⁵ However, we have shown that upon ER stress, *PLK2* is a pro-apoptotic gene. We also showed that under basal conditions, *PLK2* localizes to the ER. *PLK2* has been reported to phosphorylate proteins localized on the ER (*Grp94* and *calumenin*³⁸) and may regulate their functions. Interestingly, the subcellular localization of both *PTP4A1* and *PLK2* are altered upon ER stress, possibly because these proteins have a specific function at these sites in response to ER stress.

We confirmed previous reports that expression of $\Delta 1stTAD$ -p53 is induced following cytotoxic stresses such as nutrient deprivation and ER stress.^{11,14} The fact that $\Delta 1stTAD$ -p53 as well as its target genes are both regulated by ER stress suggests that the $\Delta 1stTAD$ -p53 downstream pathway and the ER stress pathway functionally overlap. We found that $\Delta 1stTAD$ -p53 induces genes that enhance (*PLK2*) and repress (*PTP4A1*) ER stress-induced apoptosis. It has been reported that p53 induces both pro-apoptotic genes such as *Noxa* or *Puma* and anti-apoptotic genes such as *p21* depending on the stress levels the cells have suffered. $\Delta 1stTAD$ -p53 may also induce different sets of genes to enhance or repress apoptosis according to the stress levels.

Finally, *RPS27L* was previously shown to function in ribosomal stress.³⁹ Disruption of the endogenous *RPS27L* results in activation of p53 through an increase in the binding of *Mdm2* to ribosomal proteins and a consequent decrease in p53 degradation.³⁹ Because $\Delta 1stTAD$ -p53 lacks the N-terminal *Mdm2* binding domain, it is expected that *RPS27L* should effect only FL-p53 and not $\Delta 1stTAD$ -p53. *RPS27L* is itself induced by either FL-p53 or $\Delta 1stTAD$ -p53, so we might expect that this induction leads to an alteration in the relative abundance of endogenous FL-p53 and $\Delta 1stTAD$ -p53.

In this paper, we have analyzed three novel $\Delta 1stTAD$ -p53 target genes. These genes are also targets of FL-p53, and their transcription depends on the 2nd TAD of p53. We also identified several other potential $\Delta 1stTAD$ -p53-specific target genes involved in cell cycle regulation by the BTG of family proteins and *HIPPO* signaling. These and other $\Delta 1stTAD$ -p53-specific target genes should be analyzed next to further elucidate 2nd TAD-specific functions.

ACKNOWLEDGMENTS

We thank Dr Hitoshi Kurumizaka for mentoring S. Suzuki at Waseda University. We thank Dr Marc Lamphier for critical reading of the manuscript. This study was partly supported by a Grant-in-Aid for Scientific Research (B) (#17H03587) (RO), a Grant-in-Aid for Young Scientists (B) (#19K16732) (YC) from the Ministry of Education, Culture, Sports, Science and Technology of Japan, research grants from the Applied Research for Innovative Treatment of Cancer from the Ministry of Health, Labour and Welfare (RO), P-Direct and P-Create from the Japan Agency for Medical Research and Development (RO), and research grants from the Research Grant of the Princess Takamatsu Cancer Research Fund (RO) and the Mitsubishi Foundation (to RO).

DISCLOSURE

The authors have no financial relationships to disclose.

ORCID

Rieko Ohki  <https://orcid.org/0000-0002-7775-6653>

REFERENCES

- Levine AJ, Oren M. The first 30 years of p53: growing ever more complex. *Nat Rev Cancer*. 2009;9:749-758.
- Vousden KH, Prives C. Blinded by the light: the growing complexity of p53. *Cell*. 2009;137:413-431.
- Biegging KT, Mello SS, Attardi LD. Unravelling mechanisms of p53-mediated tumour suppression. *Nat Rev Cancer*. 2014;14:359-370.

4. Sullivan KD, Galbraith MD, Andryszk Z, Espinosa JM. Mechanisms of transcriptional regulation by p53. *Cell Death Differ*. 2018;25:133-143.
5. Venot C, Maratrat M, Sierra V, Conseiller E, Debussche L. Definition of a p53 transactivation function-deficient mutant and characterization of two independent p53 transactivation subdomains. *Oncogene*. 1999;18:2405-2410.
6. Bourdon JC, Fernandes K, Murray-Zmijewski F, et al. p53 isoforms can regulate p53 transcriptional activity. *Genes Dev*. 2005;19:2122-2137.
7. Yin Y, Stephen CW, Luciani MG, Fahraeus R. p53 Stability and activity is regulated by Mdm2-mediated induction of alternative p53 translation products. *Nat Cell Biol*. 2002;4:462-467.
8. Courtois S, Verhaegh G, North S, et al. DeltaN-p53, a natural isoform of p53 lacking the first transactivation domain, counteracts growth suppression by wild-type p53. *Oncogene*. 2002;21:6722-6728.
9. Ghosh A, Stewart D, Matlashewski G. Regulation of human p53 activity and cell localization by alternative splicing. *Mol Cell Biol*. 2004;24:7987-7997.
10. Ray PS, Grover R, Das S. Two internal ribosome entry sites mediate the translation of p53 isoforms. *EMBO Rep*. 2006;7:404-410.
11. Candeias MM, Powell DJ, Roubalova E, et al. Expression of p53 and p53/47 are controlled by alternative mechanisms of messenger RNA translation initiation. *Oncogene*. 2006;25:6936-6947.
12. Ohki R, Kawase T, Ohta T, Ichikawa H, Taya Y. Dissecting functional roles of p53 N-terminal transactivation domains by microarray expression analysis. *Cancer Sci*. 2007;98:189-200.
13. Zhu J, Zhang S, Jiang J, Chen X. Definition of the p53 functional domains necessary for inducing apoptosis. *J Biol Chem*. 2000;275:39927-39934.
14. Bourougaa K, Naski N, Boularan C, et al. Endoplasmic reticulum stress induces G2 cell-cycle arrest via mRNA translation of the p53 isoform p53/47. *Mol Cell*. 2010;38:78-88.
15. Brady CA, Jiang D, Mello SS, et al. Distinct p53 transcriptional programs dictate acute DNA-damage responses and tumor suppression. *Cell*. 2011;145:571-583.
16. Jiang D, Brady CA, Johnson TM, et al. Full p53 transcriptional activation potential is dispensable for tumor suppression in diverse lineages. *Proc Natl Acad Sci U S A*. 2011;108:17123-17128.
17. Maier B, Gluba W, Bernier B, et al. Modulation of mammalian life span by the short isoform of p53. *Genes Dev*. 2004;18:306-319.
18. Phang BH, Othman R, Bougeard G, et al. Amino-terminal p53 mutations lead to expression of apoptosis proficient p47 and prognosticate better survival, but predispose to tumorigenesis. *Proc Natl Acad Sci U S A*. 2015;112:E6349-E6358.
19. Lambert PF, Kashanchi F, Radonovich MF, Shiekhattar R, Brady JN. Phosphorylation of p53 serine 15 increases interaction with CBP. *J Biol Chem*. 1998;273:33048-33053.
20. Li AG, Piluso LG, Cai X, Gadd BJ, Ladurner AG, Liu X. An acetylation switch in p53 mediates holo-TFIID recruitment. *Mol Cell*. 2007;28:408-421.
21. Ohki R, Nemoto J, Murasawa H, et al. Reprimo, a new candidate mediator of the p53-mediated cell cycle arrest at the G2 phase. *J Biol Chem*. 2000;275:22627-22630.
22. Asano Y, Kawase T, Okabe A, et al. IER5 generates a novel hypo-phosphorylated active form of HSF1 and contributes to tumorigenesis. *Sci Rep*. 2016;6:19174.
23. Chen Y, Takikawa M, Tsutsumi S, et al. PHLDA1, another PHLDA family protein that inhibits Akt. *Cancer Sci*. 2018;109:3532-3542.
24. Kawase T, Ohki R, Shibata T, et al. PH domain-only protein PHLDA3 is a p53-regulated repressor of Akt. *Cell*. 2009;136:535-550.
25. Burns TF, Fei P, Scata KA, Dicker DT, El-Deiry WS. Silencing of the novel p53 target gene Snk/Plk2 leads to mitotic catastrophe in paclitaxel (taxol)-exposed cells. *Mol Cell Biol*. 2003;23:5556-5571.
26. Min SH, Kim DM, Heo YS, et al. New p53 target, phosphatase of regenerating liver 1 (PRL-1) downregulates p53. *Oncogene*. 2009;28:545-554.
27. He H, Sun Y. Ribosomal protein S27L is a direct p53 target that regulates apoptosis. *Oncogene*. 2007;26:2707-2716.
28. Li J, Tan J, Zhuang L, et al. Ribosomal protein S27-like, a p53-inducible modulator of cell fate in response to genotoxic stress. *Cancer Res*. 2007;67:11317-11326.
29. Oda K, Arakawa H, Tanaka T, et al. p53AIP1, a potential mediator of p53-dependent apoptosis, and its regulation by Ser-46-phosphorylated p53. *Cell*. 2000;102:849-862.
30. Taira N, Nihira K, Yamaguchi T, Miki Y, Yoshida K. DYRK2 is targeted to the nucleus and controls p53 via Ser46 phosphorylation in the apoptotic response to DNA damage. *Mol Cell*. 2007;25:725-738.
31. Zhu J, Zhou W, Jiang J, Chen X. Identification of a novel p53 functional domain that is necessary for mediating apoptosis. *J Biol Chem*. 1998;273:13030-13036.
32. Townsend PA, Scarabelli TM, Davidson SM, Knight RA, Latchman DS, Stephanou A. STAT-1 interacts with p53 to enhance DNA damage-induced apoptosis. *J Biol Chem*. 2004;279:5811-5820.
33. Trainor CD, Mas C, Archambault P, Di Lello P, Omichinski JG. GATA-1 associates with and inhibits p53. *Blood*. 2009;114:165-173.
34. Bessette DC, Qiu D, Pallen CJ. PRL PTPs: mediators and markers of cancer progression. *Cancer Metastasis Rev*. 2008;27:231-252.
35. Rios P, Li X, Kohn M. Molecular mechanisms of the PRL phosphatases. *FEBS J*. 2013;280:505-524.
36. Bai Y, Luo Y, Liu S, et al. PRL-1 protein promotes ERK1/2 and RhoA protein activation through a non-canonical interaction with the Src homology 3 domain of p115 Rho GTPase-activating protein. *J Biol Chem*. 2011;286:42316-42324.
37. Sacchetti C, Bai Y, Stanford SM, et al. PTP4A1 promotes TGFbeta signaling and fibrosis in systemic sclerosis. *Nat Commun*. 2017;8:1060.
38. Salvi M, Trashi E, Cozza G, Franchin C, Arrigoni G, Pinna LA. Investigation on PLK2 and PLK3 substrate recognition. *Biochim Biophys Acta*. 2012;1824:1366-1373.
39. Xiong X, Zhao Y, Tang F, et al. Ribosomal protein S27-like is a physiological regulator of p53 that suppresses genomic instability and tumorigenesis. *Elife*. 2014;3:e02236.

SUPPORTING INFORMATION

Additional supporting information may be found online in the Supporting Information section.

How to cite this article: Suzuki S, Tsutsumi S, Chen Y, et al. Identification and characterization of the binding sequences and target genes of p53 lacking the 1st transactivation domain. *Cancer Sci*. 2020;111:451-466. <https://doi.org/10.1111/cas.14279>